Combined Effect of Phenoxy and Carboxylate Bridges on Magnetic Properties of a Series of Macrocyclic Dinickel(II) Complexes

Kausik K. Nanda,[1] Ramprasad Das,[1] Laurence K. Thompson,[2] Krishnan Venkatsubramanian,[3,4] and Kamalaksha Nag*,[1]

Department of Inorganic Chemistry, Indian Association for the Cultivation of Science, Calcutta 700 032, India, Department of Chemistry, Memorial University of Newfoundland, St. John's, Newfoundland, Canada A1B 3X7, and Coordination Chemistry Discipline, Central Salt and Marine Chemicals Research Institute, Bhavnagar 364 002, India

Received January 27, 1994[⊗]

A series of binuclear nickel(II) complexes with one carboxylate bridge and two phenoxy bridges have been synthesized from a tetraamino diphenol macrocyclic ligand H_2L. The perchlorate salts of the complex cation $[Ni_2L(\mu\text{-}O_2CR)(H_2O)_2]^+$ (R = H, CH_3, C_2H_5, C_3H_8, or C_6H_5) have been spectroscopically characterized. All the complexes undergo reversible one-electron oxidation (CH_3CN/Pt) at $E_{1/2}(1) = 0.80$ V *vs* Ag/AgCl. Further oxidation of the butyrate and benzoate complexes take place nearly reversibly at $E_{1/2}(2) = 0.97$ V. The crystal structure of $[Ni_2L(\mu\text{-}O_2CCH_3)(H_2O)_2](ClO_4)\cdot CH_3OH\cdot H_2O$ has been determined: monoclinic, space group $P2_1/n$; $a = 10.621(1)$ Å, $b = 22.375(2)$ Å, $c = 14.411(2)$ Å, $\beta = 107.39(1)°$, $Z = 4$. The structure was solved by direct methods and refined to $R = 0.049$ and $R_w = 0.056$. Variable-temperature (5-300 K) magnetic susceptibility measurements of the compounds show that they exhibit weak Ni···Ni exchange interactions. The exchange coupling constant (J) varies in the following way: formate, -0.7 cm^{-1}; acetate, 2.9 cm^{-1}; propionate, 2.2 cm^{-1}; butyrate, 0.5 cm^{-1}; and benzoate, 5.0 cm^{-1}.

Introduction

The occurrence of a pair of nickel(II) centers in the active site of the hydrolytic enzyme urease[5] of both plant[6] (jack bean) and microbial[7] (*Klebsiella aerogenes*) origin has aroused considerable interest in the chemistry of binuclear nickel(II) complexes. Urease hydrolyses urea to ammonia and carbamate, which spontaneously degrades to carbon dioxide and a second molecule of ammonia. As yet no definite picture has emerged for the coordination environment around nickel in the active site. Nevertheless, the electronic absorption spectra and EXAFS data seem to suggest[8] an octahedral geometry for the metal centers with nitrogen and oxygen donors. The magnetic behavior of urease is intriguing and conflicting results have been reported.[9-11] For example, from variable-temperature magnetic susceptibility measurements of jack bean urease it has been proposed[9] that 80% of the nickel(II) ions are antiferromagnetically coupled ($J = -6.3$ cm^{-1}), while the remaining 20% are isolated high-spin ($S = 1$) nickel. In contrast, a saturation magnetization study[10] has indicated the absence of Ni-Ni exchange interaction. On the other hand, the presence of a mixture of both antiferromagnetically (major fraction) and ferromagnetically (minor fraction) coupled nickel(II) centers has been suggested[11] on the basis of variable-temperature MCD measurements.

Synthetic models[12-16] have addressed ligand environment and magnetic and electronic properties of the nickel(II) pair in urease. These compounds contain either two[12-15] or three[16] carboxylate bridges. The dicarboxylate bridged complexes additionally contain an aqua,[12] hydroxy,[13] or phenoxy[14,15] bridge. All of them, however, exhibit weak antiferromagnetic interactions.

We have recently reported[17] magnetostructural relationships in a series of binuclear nickel(II) complexes derived from the macrocyclic ligand H_2L. A wide variation of the exchange parameter (J) ranging between -1 and -67 cm^{-1} has been accomplished[17a] by changing the stereochemistry and auxiliary axial ligands. For the complexes with centrosymmetric structures it has been shown[17b] that the value of $-J$ increases linearly with the increase of Ni-O(phenoxy)-Ni bridge angle or intramolecular Ni···Ni separation. We report here the variable-temperature magnetic behavior and electrochemical properties of a series of monocarboxylato-bridged dinickel(II) complexes, $[Ni_2L(\mu\text{-}O_2CR)(H_2O)_2](ClO_4)\cdot$solvent, along with the structure of the acetate complex.

⊗ Abstract published in *Advance ACS Abstracts,* October 15, 1994.

(1) Indian Association for the Cultivation of Science.
(2) Memorial University of Newfoundland.
(3) Central Salt and Marine Chemicals Research Institute.
(4) Deceased, November 22, 1993.
(5) (a) Andrews, R. W.; Blakeley, R. L.; Zerner, B. In *The Bioinorganic Chemistry of Nickel*; Lancaster, J. R., Jr., Ed.; VCH Publishers: New York, 1988; p 141. (b) Mobley, H. L. T.; Hausinger, R. P. *Microbiol. Rev.* **1989**, *53*, 85. (c) Todd, M. J.; Hausinger, R. P. *J. Biol. Chem.* **1989**, *264*, 15835.
(6) (a) Dixon, N. E.; Gazzola, C.; Watters, J. J.; Blakeley, R. W.; Zerner, B. *J. Am. Chem. Soc.* **1975**, *97*, 4130. Blakerley, R. L.; Zerner, B. *J. Mol. Catal.* **1984**, *23*, 263.
(7) Todd, M. J.; Hausinger, R. P. *J. Biol. Chem.* **1987**, *262*, 5963.
(8) (a) Blakeley, R. L.; Dixon, N. E.; Zerner, B. *Biochim. Biophys. Acta* **1983**, *744*, 219. (b) Alagna, L.; Hasnaim, S. S.; Piggot, B.; Williams, D. J. *Biochem. J.* **1984**, *220*, 590. (c) Clark, P. A.; Wilcox, D. E.; Scott, R. A. *Inorg. Chem.* **1990**, *29*, 579.
(9) Clark, P. A.; Wilcox, D. E. *Inorg. Chem.* **1989**, *28*, 1326.
(10) Day, E. P.; Peterson, J.; Sendova, M. S.; Todd, M. J.; Hausinger, R. P. *Inorg. Chem.* **1993**, *32*, 634.
(11) Finnegan, M. G.; Kowai, A. T.; Werth, M. T.; Clark, P. A.; Wilcox, D. E.; Johnson, M. K. *J. Am. Chem. Soc.* **1991**, *113*, 4030.
(12) Terpeimen, U.; Hamalainen, R.; Reedijk, J. *Polyhedron* **1987**, *6*, 1603.
(13) Chaudhuri, P.; Kuppers, H.-J.; Wieghardt, K.; Gehring, S.; Haase, W.; Nuber, B.; Weiss, J. *J. Chem. Soc., Dalton Trans.* **1988**, 1367.
(14) Buchanan, R. M.; Mashuta, M. S.; Oberhausen, K. J.; Richardson, J. F.; Li, Q.; Hendrickson, D. N. *J. Am. Chem. Soc.* **1989**, *111*, 4497.
(15) Holman, T. R.; Hendrich, M. P.; Que, L., Jr. *Inorg. Chem.* **1992**, *31*, 937.
(16) Wages, H. E.; Taft, K. L.; Lippard, S. J. *Inorg. Chem.* **1993**, *32*, 4985.
(17) (a) Nanda, K. K.; Das, R.; Thompson, L. K.; Venkatsubramanian, K.; Paul, P.; Nag, K. *Inorg. Chem.* **1994**, *33*, 1188. (b) Nanda, K. K.; Thompson, L. K.; Bridson, J. N.; Nag, K. *J. Chem. Soc., Chem. Commun.* **1994**, 1337.

0020-1669/94/1333-5934$04.50/0

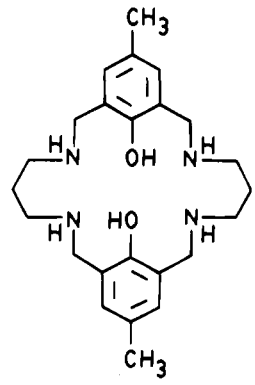

H_2L

Experimental Section

Materials. All chemicals were reagent grade and used as received. The macrocyclic ligand H_2L[18] and the precursor complex $[Ni_2L(CH_3OH)_2(ClO_4)_2]\cdot 2NH(C_2H_5)_3ClO_4$[19] were prepared as reported earlier.

Synthesis of $[Ni_2L(\mu\text{-}O_2CH)(H_2O)_2](ClO_4)$ (**1**), $[Ni_2L(\mu\text{-}O_2CCH_3)(H_2O)_2](ClO_4)\cdot CH_3OH\cdot H_2O$ (**2**), $[Ni_2L(\mu\text{-}O_2CCH_2CH_3)(H_2O)_2](ClO_4)\cdot 2CH_3CH_2CO_2H$ (**3**), $[Ni_2L(\mu\text{-}O_2CCH_2CH_2CH_3)(H_2O)_2](ClO_4)\cdot 2CH_3CH_2CH_2CO_2H$ (**4**), and $[Ni_2L(\mu\text{-}O_2CC_6H_5)(H_2O)_2](ClO_4)\cdot 2C_6H_5CO_2H$ (**5**). All of these complexes were prepared in the same way as illustrated below for complex **3**, which is typical of the series.

A methanol solution (20 mL) of $[Ni_2L(CH_3OH)_2(ClO_4)_2]\cdot 2NH(C_2H_5)_3ClO_4$ (1.19 g, 1 mmol) was treated with propionic acid (0.30 g, 4 mmol). The wine red solution that changed to blue color in 0.5 h was allowed to evaporate slowly for 24 h. The sky blue crystals deposited were collected by filtration and washed first with a small portion of ice-cooled ethanol–water (1:1) mixture and then with diethyl ether. The yield for **3** was *ca.* 60%, and for the others varied between 70% (**1**, **2**) and 60% (**4**, **5**).

Anal. Calcd for $C_{25}H_{39}N_4O_{10}ClNi_2$ (**1**): C, 42.38; H, 5.01; N, 7.91. Found: C, 41.97; H, 5.12; N, 7.88. Calcd for $C_{27}H_{47}N_4O_{12}ClNi_2$ (**2**): C, 41.98; H, 6.09; N, 7.25. Found: C, 42.32; H, 5.93; N, 7.12. Calcd for $C_{33}H_{55}N_4O_{14}ClNi_2$ (**3**): C, 44.80; H, 6.22; N, 6.34. Found: C, 45.31; H, 6.25; N, 6.16. Calcd for $C_{36}H_{61}N_4O_{14}ClNi_2$ (**4**): C, 46.66; H, 6.59; N, 6.05. Found: C, 46.14; H, 6.65; N, 6.17. Calcd for $C_{45}H_{55}N_4O_{14}ClNi_2$ (**5**): C, 52.53; H, 5.35; N, 5.45. Found: C, 52.87, H, 5.23; N, 5.69. C, H, and N analyses were performed on a Perkin–Elmer 240C elemental analyzer.

Physical Measurements. Infrared spectra were recorded on a Perkin-Elmer 783 spectrophotometer using KBr disks. Electronic spectra were obtained with Shimadzu UV2100 and Hitachi U3400 spectrophotometers over the UV–vis and near-IR regions. Conductivity measurements were carried out using a Philips PR9500 conductivity bridge. The electrochemical measurements were performed at room temperature in acetonitrile under O_2-free conditions using a BAS 100B electrochemical analyzer (Bioanalytical Systems). A three-electrode assembly (BAS) comprising of a Pt working electrode, Pt auxiliary electrode, and a Ag/AgCl reference electrode was used. The supporting electrolyte was tetraethylammonium perchlorate (0.1 M), and all solutions in acetonitrile were *ca.* 1 mM in complex.

Variable-temperature magnetic susceptibility data were obtained in the range 5–300 K by using an Oxford Instruments superconducting Faraday magnetic susceptibility system with a Sartorius 4432 microbalance. A main solenoid field at 1.5 T and a gradient field of 10 T m^{-1} were employed. Susceptibility data were corrected for diamagnetism using Pascal constants. $Hg[Co(NCS)_4]$ was used as a calibration standard.

X-ray Crystallography. Crystals of $[Ni_2L(\mu\text{-}O_2CCH_3)(H_2O)_2](ClO_4)\cdot CH_3OH\cdot H_2O$ (**2**) were obtained by diffusion of diethyl ether to a methanol solution of the complex. The diffraction intensities were collected by using a Enraf-Nonius CAD4 diffractometer with graphite monochromated Mo Kα radiation (λ = 0.710 69 Å). The unit cell parameters were obtained by least-squares refinement of 25 arbitrarily chosen higher-order reflections. Crystal stabilities were chequed by monitoring intensities of three standard reflections after every 100, and no significant variations were observed. The intensity data were corrected for Lorentz polarization effects and for absorption (transmission varied between 99.2% and 92.2%) by an empirical method.[20] A total of 5080 reflections were collected in the 2θ range 2–50°, of which 3975 reflections with $I > 3\sigma(I)$ were used for structure determination. The structure was solved by direct and Fourier difference methods using the program MULTAN 82[21] and the SDP package[22] for the PDP-11/73 system. Hydrogen atoms were generated using stereochemical constraints. The structure was refined by block-diagonal least-squares technique to final residuals of R and R_w of 0.049 and 0.056, respectively, using a unit weighting scheme.[23] The scattering factors were taken from ref 24. The final difference map showed ripples of 0.36 e $Å^{-3}$ around the heavy atoms. A summary of crystal data is given in Table 1. Anisotropic thermal parameters (Table SI), hydrogen atom positions (Table SII), and a full list of bond lengths and angles (Table SIII) are included as supplementary material.

Table 1. Summary of Crystal Data for $[Ni_2L(\mu\text{-}O_2CCH_3)(H_2O)_2](ClO_4)\cdot CH_3OH\cdot H_2O$ (**2**)

formula	$C_{27}H_{47}N_4O_{12}ClNi_2$
f_w	772.52
cryst system	monoclinic
space group	$P2_1/n$
a, Å	10.621(1)
b, Å	22.375(2)
c, Å	14.411(2)
β, deg	107.39(1)
V, Å^3	3268.2(4)
Z	4
d_{calcd}, g cm^{-3}	1.570
Cryst dimension, mm	0.24 × 0.21 × 0.16
λ(Mo Kα), Å	0.710 69
μ, cm^{-1}	12.90
temp, K	293
R^a	0.049
R_w^b	0.056

^{a} $R = \sum|F_o - F_c|/\sum F_o$. ^{b} $R_w = [\sum w(F_o - F_c)^2/\sum wF_o^2]^{1/2}$.

Results and Discussion

Characterization. The monocarboxylate-bridged dinickel(II) complexes having the composition $[Ni_2L(\mu\text{-}O_2CR)(H_2O)_2](ClO_4)\cdot$solvent (R = H (**1**) or CH_3 (**2**)) and $[Ni_2L(\mu\text{-}O_2CR)(H_2O)_2](ClO_4)\cdot 2RCO_2H$ (R = C_2H_5 (**3**), C_3H_7 (**4**), or C_6H_5 (**5**)) were obtained by reacting the precursor complex $[Ni_2L(CH_3OH)_2(ClO_4)_2]\cdot 2NH(C_2H_5)_3ClO_4$ with appropriate carboxylic acids. The inclusion of two molecules of the free carboxylic acids in **3**–**5** is a typical feature of these complexes and occurs even when 1 equiv of the precursor complex is treated with only 2 equiv of the acid, of course, in reduced yield. Attempts to prepare the dicarboxylate-bridged complexes by reacting the monocarboxylates with excess of sodium salt of the carboxylic acids were unsuccessful. The reaction involving $Ni(CH_3CO_2)_2\cdot 4H_2O$ and H_2L, on the other hand, afforded a nonelectrolytic complex of composition $[Ni_2L(OAc)_4]\cdot 2CH_3OH\cdot 2H_2O$ which appears to contain bidentate chelating acetate group. This compound, however, was not studied in detail.

(18) (a) Mandal, S. K.; Nag, K. *J. Org. Chem.* **1986**, *51*, 3900. (b) Mandal, S. K.; Thompson, L. K.; Nag, K.; Charland, J.-P.; Gabe, E. J. *Inorg. Chem.* **1987**, *26k*, 1391.

(19) Das, R.; Nag, K. *Inorg. Chem.* **1991**, *30*, 2831.

(20) North, A. C. T.; Phillips, D. C.; Mathews, F. S. *Acta Crystallogr., Sect. A* **1968**, *24*, 351.

(21) Main, P.; Germain, G.; Declereq, J. P.; Woolfson, M. M.; MULTAN-82. A System of Computer Programs for the Automatic solution of Crystal Structures from X-ray Data. University of York, York, U.K. 1982.

(22) Enraf-Nonius Structure Determination Package, Enraf-Nonius, Delft, The Netherlands, 1985.

(23) Dunitz, J. D.; Seiler, P. *Acta Crystallogr., Sect. B* **1973**, *29*, 589.

(24) *International Table for X-Ray Crystallography*; Kynoch Press: Birmingham, England, 1974; Vol. IV.

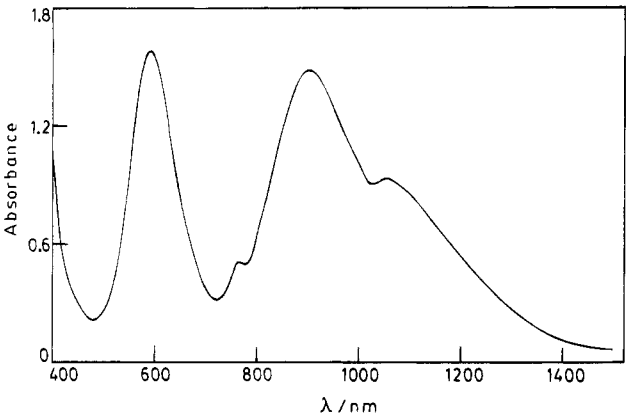

Figure 1. Visible spectrum of **3** in acetonitrile (1.01×10^{-2} M).

Table 2. Infrared[a] and Electronic[b] Spectral Data for Complexes **1**–**5**

complex	IR, cm^{-1}	γ_{max}, nm (ϵ, M^{-1} cm^{-1})
1	3400, 3250, 3225, 2720, 1590, 1370, 1100, 625	1070 (10), 890 (20), 760 (6), 588 (15), 348 (sh)
2	3400, 3260, 3220, 1570, 1360, 1100, 630	1050 (11), 900 (23), 760 (sh), 587 (17), 350 (sh)
3	3400, 3260, 3240, 1670, 1570, 1370, 1100, 630	1070 (10), 900 (16), 760 (6), 587 (17), 350 (sh)
4	3400, 3260, 3230, 1670, 1570, 1370, 1100, 625	1100 (12), 890 (15), 760 (6), 600 (17), 350 (sh)
5	3400, 3260, 3220, 1650, 1590, 1380, 1100, 620	1080 (11), 900 (17), 760 (7), 590 (23), 350 (sh)

[a] In KBr. [b] In CH_3CN.

Infrared spectra of the complexes are diagnostic in regions associated with the NH stretch of L^{2-}, C=O and C-O stretches carboxylic acids, and the Cl—O stretch of ClO_4^- (Table 2). A broad band centered at 3400 cm^{-1} is observed due to the water molecules. The NH stretch in all the cases is split and are observed at about 3260 and 3230 cm^{-1}. The splitting of the NH band can be associated either to the involvement of one of the NH groups in hydrogen bonding (see crystal structure) or to crystal packing effects. The ionic nature of perchlorate is evident from the presence of a broad band around 1100 cm^{-1}. More importantly, complexes **3**–**5** can be distinguished from **1** and **2** by noting the occurrence of a medium intensity band at *ca.* 1660 cm^{-1} due to ν(C=O) of the free carboxylic acids present as dimers:[25]

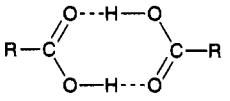

All the complexes, however, exhibit $\nu_{as}(CO_2^-)$ and $\nu_s(CO_2^-)$ due to the bridged carboxylate moiety[26] at about 1570 and 1360 cm^{-1}, respectively. Complex **1** is further characterized by a sharp band at 2720 cm^{-1} due to the CH stretch of the formate.

Electronic absorption spectra of **1**–**5** in both the solid state (Nujol mull) and solution (acetonitrile) are closely comparable, indicating similar chromophores in both physical states. A typical solution spectrum for **3** in the visible region is shown in Figure 1. All the complexes exhibit (Table 2) five absorption bands at about 1050, 900, 760, 590, and 350 nm, which are indicative of low symmetry six-coordinate geometries.[27] The

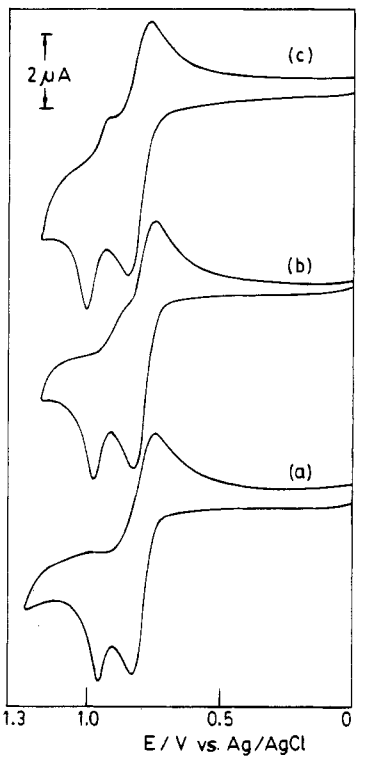

Figure 2. Cyclic voltammograms of complexes **2** (a), **3** (b), and **4** (c) in acetonitrile with Pt electrode at a scan rate of 50 mV s^{-1}.

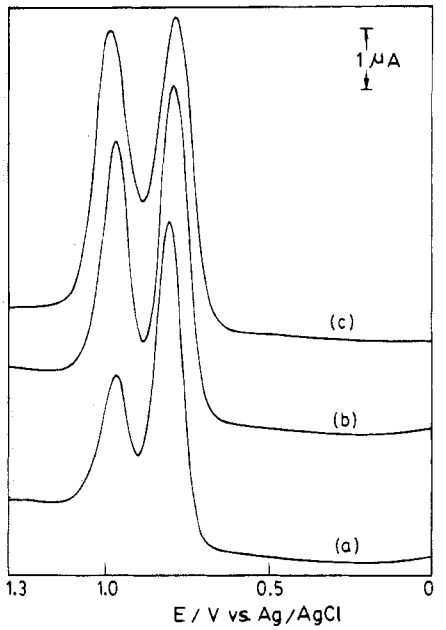

Figure 3. Differential pulse voltammograms of complexes **1** (a), **5** (b), and **4** (c) in acetonitrile with a Pt electrode. Conditions: pulse amplitude, 50 mV; scan rate, 20 mV s^{-1}.

first two bands appear to be the split components of the spin-allowed $^3A_{2g} \rightarrow {}^3T_{2g}$ transition of octahedral nickel(II), which in D_{4h} symmetry may be attributed to $^3B_{1g} \rightarrow {}^3E_g$ and $^3B_{1g} \rightarrow {}^3B_{2g}$ transitions. The band at 760 nm is very weak and probably due to the spin-forbidden $^3A_{2g} \rightarrow {}^1E_g$ transition. The remaining two bands are $^3A_{2g} \rightarrow {}^3T_{1g}$ and $^3A_{2g} \rightarrow {}^3T_{1g}(P)$ transitions. Indeed, in agreement with the spectroscopic data the crystal structure of **2** (see later) shows that the two nickel(II) centers are in distorted octahedral environment with relatively long, axial Ni—OH_2 bonds.

Electrochemistry. The cyclic voltammograms for complexes **2**–**4** and differential pulse voltammograms for **1**, **4**, and **5** with

(25) Bellamy, L. J. *Infrared Spectra of Complex Molecules*, 3rd ed.; Chapman & Hall: London, 1975.
(26) Nakamoto, K. *Infrared and Raman Spectra of Inorganic and Coordination Compounds*, 3rd ed.; John Wiley & Sons: New York, 1978.
(27) Lever, A. B. P. *Inorganic Electronic Spectroscopy*; 2nd ed.; Elsevier: Amsterdam, 1984.

Table 3. Electrochemical Data[a] for Oxidation of Complexes **1**–**5**

	$Ni^{II}Ni^{II}/Ni^{II}Ni^{III}$		$Ni^{II}Ni^{III}/Ni^{III}Ni^{III}$		
complex	$E_{1/2}(1)$[b]	E_p[c]	$E_{1/2}(2)$[b]	ΔE_p[c]	10^{-2} K_{com}
1	0.81	90	1.0[d]		
2	0.79	80	0.96[d]		
3	0.79	80	0.98[d]		
4	0.81	70	0.97	75	5.1
5	0.79	80	0.96	90	7.5

[a] Potential in V *vs* Ag/AgCl. [b] $E_{1/2} = 0.5(E_{p,c} + E_{p,a})$ at scan rate of 50 mV s^{-1}. [c] $\Delta E_p = E_{p,c} - E_{p,a}$ at scan rate of 50 mV s^{-1}. [d] Irreversible process.

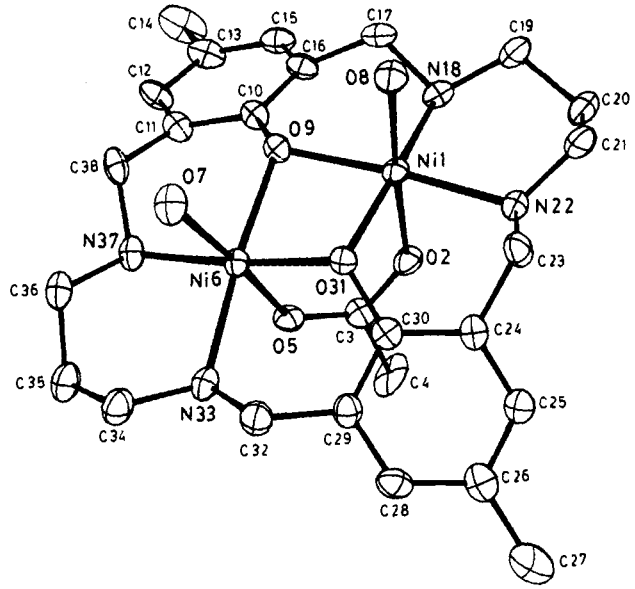

Figure 4. ORTEP view of $[Ni_2L(\mu\text{-}O_2CCH_3)(H_2O)_2](ClO_4)\cdot CH_3OH\cdot H_2O$ (**2**).

regard to their oxidation behavior in acetonitrile (platinum electrodes) are shown in Figures 2 and 3, respectively. The electrochemical data for the complexes are given in Table 3. All the complexes undergo one electron oxidation to $Ni^{II}Ni^{III}$ species, almost reversibly, at about 0.8 V *vs* Ag/AgCl. However, as may be seen in Figure 2 that although a second anodic wave due to the formation of the $Ni^{III}Ni^{III}$ occurs for all the complexes, the return wave is absent in **2**, barely visible in **3**, but clearly present in **4** for which the redox couple is reversible. A similar trend is also observed in Figure 3 in which the pulse heights of the two oxidation steps are equal for **4**, nearly equal for **5**, but approximately in the ratio 1:0.5 for **1**. Clearly, the heterogeneous electron transfer rate constants for the second oxidation step vary considerably among the complexes. On the other hand, the electrochemical data given in Table 3 reveal that the oxidation potentials of the complexes are not significantly affected by the change of the carboxylic acids. It should be noted that similar to **4** and **5**, the precursor complex, $[Ni_2L(CH_3OH)_2(ClO_4)_2]\cdot 2NH(C_2H_5)_3ClO_4$ also undergoes stepwise oxidations at $E_{1/2}(1) = 0.94$ V and $E_{1/2}(2) = 1.08$ V.[19] The easier oxidation of **4** and **5** relative to the precursor complex may be attributed to the electron-rich carboxylate bridge, which stabilizes the higher oxidation state.

The stability of the mixed-valence $Ni^{II}Ni^{III}$ species can be expressed in terms of the comproportionation constant, K_{com}[28]

$$Ni^{II}Ni^{II} + Ni^{III}Ni^{III} \overset{K_{com}}{\rightleftharpoons} 2Ni^{II}Ni^{III}$$

$$K_{com} = \exp(nF|E_{1/2}(1) - E_{1/2}(2)|/RT)$$

Low values of K_{com}, 5.1×10^2 for **4** and 7.5×10^2 for **5**, imply lesser stability of the mixed-valence species and hence easier access to the formation of the dinickel(III) species.

Table 4. Atomic Positional Parameters and Equivalent Isotropic Thermal Parameters for $[Ni_2L(\mu\text{-}O_2CCH_3)(H_2O)_2](ClO_4)\cdot CH_3OH\cdot H_2O$ (**2**)

atom	*x*	*y*	*z*	B,[a] Å^2
Ni(1)	0.62411(7)	0.02609(3)	0.77457(5)	2.06(2)
Ni(6)	0.81725(7)	−0.04271(3)	0.69578(5)	2.07(2)
Cl(39)	0.3829(2)	0.2312(1)	0.6093(1)	5.00(5)
O(2)	0.7477(4)	−0.0115(2)	0.8978(3)	2.7(1)
O(5)	0.9027(4)	−0.0537(2)	0.8434(3)	2.6(1)
O(7)	0.7398(4)	−0.0325(2)	0.5406(3)	3.4(1)
O(8)	0.4825(4)	0.0620(2)	0.6478(3)	3.0(1)
O(9)	0.7683(4)	0.0458(2)	0.7104(3)	2.18(9)
O(31)	0.6208(4)	−0.0573(2)	0.6986(3)	2.15(9)
O(40)	0.2893(7)	0.2634(3)	0.5391(5)	7.7(2)
O(41)	0.347(1)	0.1721(4)	0.6104(8)	12.1(4)
O(42)	0.409(2)	0.2551(6)	0.6956(7)	20.6(7)
O(43)[b]	0.499(1)	0.2306(8)	0.590(1)	18.9(7)
O(45)[c]	0.4314(4)	−0.0641(2)	0.5185(3)	3.7(1)
O(46)	0.8261(5)	0.1007(3)	1.0855(4)	6.0(2)
N(18)	0.6453(5)	0.1054(2)	0.8533(4)	2.6(1)
N(22)	0.4733(5)	−0.0032(2)	0.8332(4)	2.4(1)
N(33)	0.8587(5)	−0.1337(2)	0.6907(4)	2.8(1)
N(37)	1.0046(5)	−0.0211(2)	0.6838(3)	2.5(1)
C(3)	0.8472(6)	−0.0431(3)	0.9083(4)	2.5(1)
C(4)	0.9042(8)	−0.0723(5)	1.0053(5)	5.7(3)
C(10)	0.8603(6)	0.0883(3)	0.7449(4)	2.2(1)
C(11)	0.9808(6)	0.0864(3)	0.7226(4)	2.5(1)
C(12)	1.0775(6)	0.1297(3)	0.7598(5)	3.3(2)
C(13)	1.0613(7)	0.1752(3)	0.8202(5)	3.3(2)
C(14)	1.1690(8)	0.2202(4)	0.8618(7)	5.3(2)
C(15)	0.9402(7)	0.1777(3)	0.8380(5)	3.1(2)
C(16)	0.8401(6)	0.1374(3)	0.8001(4)	2.6(1)
C(17)	0.7070(7)	0.1523(3)	0.8105(4)	2.9(2)
C(19)	0.5312(7)	0.1330(3)	0.8757(5)	3.5(2)
C(20)	0.4586(7)	0.0890(3)	0.9218(5)	3.8(2)
C(21)	0.3851(7)	0.0412(3)	0.8225(5)	3.8(2)
C(23)	0.4052(6)	−0.0541(3)	0.7769(5)	3.0(2)
C(24)	0.4940(6)	−0.1075(3)	0.7886(4)	2.5(1)
C(25)	0.4763(6)	−0.1556(3)	0.8437(4)	2.8(2)
C(26)	0.5556(7)	−0.2052(3)	0.8563(4)	3.1(2)
C(27)	0.5387(8)	−0.2573(3)	0.9194(5)	4.4(2)
C(28)	0.6481(6)	−0.2069(3)	0.8059(5)	3.2(2)
C(29)	0.6647(6)	−0.1598(3)	0.7483(4)	2.7(2)
C(30)	0.5971(6)	−0.1070(3)	0.7461(4)	2.3(1)
C(32)	0.7427(7)	−0.1710(3)	0.6776(5)	3.3(2)
C(34)	0.9338(7)	−0.1560(3)	0.6258(5)	3.6(2)
C(35)	1.0649(7)	−0.1243(4)	0.6448(6)	4.0(2)
C(36)	1.0523(6)	−0.0585(3)	0.6170(5)	3.2(2)
C(38)	1.0009(6)	0.0424(3)	0.6510(4)	2.9(2)
C(44)[b]	0.3621(8)	−0.1191(4)	0.5155(5)	4.6(2)

[a] Anisotropically refined atoms are given in the form of the isotropic equivalent displacement parameter defined as $^4/_3[a^2B(1,1) + b^2B(1,2) + c^2B(3,3) + ab(\cos\gamma)B(1,2) + ac(\cos\beta)B(1,3) + bc(\cos\alpha)B(2,3)]$. [b] Solvent CH_3OH. [c] Solvent H_2O.

Description of the Structure of $[Ni_2L(\mu\text{-}O_2CCH_3)(H_2O)_2](ClO_4)\cdot CH_3OH\cdot H_2O$ (2). The ORTEP representation of the complex cation $[Ni_2L(\mu\text{-}O_2CCH_3)(H_2O)_2]^+$ along with the atom labelling scheme is shown in Figure 4. Atomic coordinates and selected bond lengths and angles are given in Tables 4 and 5, respectively. The structure consists of two distorted nickel centers bridged by two phenoxide oxygens and two carboxylate oxygens of the acetate. The coordination environment NiN_2O_4 of each metal center is completed by two secondary amine nitrogen donors of the macrocyclic ligand and a water molecule *trans* axially disposed to the carboxylate oxygen. The complex molecule lacks symmetry. The adjacent donor atoms in the equatorial planes of the two metal centers are alternately displaced above and below the mean planes by

(28) Richardson, D.; Taube, H. *Coord. Chem. Rev.* **1984**, *60*, 107.

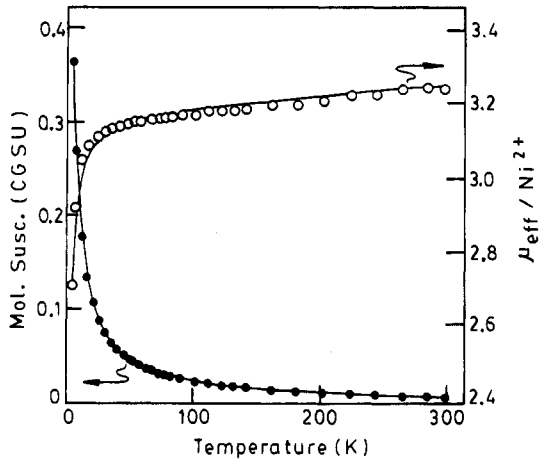

Figure 5. Molar magnetic susceptibility (χ_M) per complex molecule and effective magnetic moment per nickel(II) ion (μ_{eff}) *vs* temperature for **1**. The solid lines result from a least-squares fit to the theoretical eq 1 given in the text.

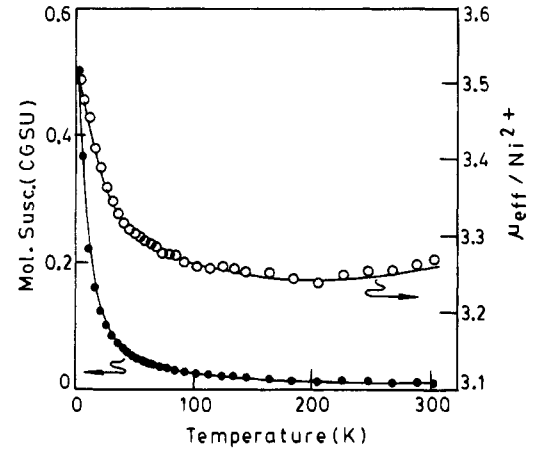

Figure 6. Molar magnetic susceptibility data (χ_M) per complex molecule and effective magnetic moment per nickel(II) ion (μ_{eff}) *vs* temperature for **2**. The solid lines result from a least squares fit to the theoretical eq 2 given in the text.

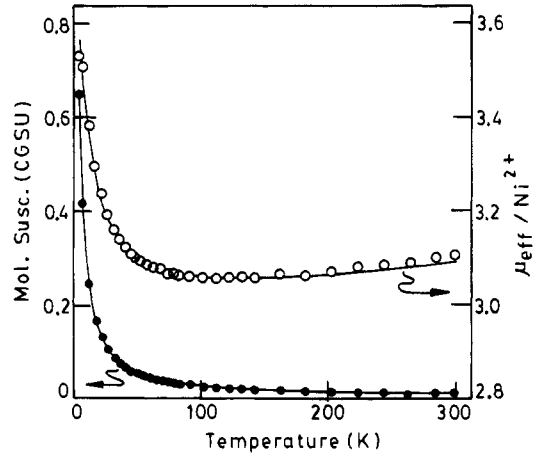

Figure 7. Molar magnetic susceptibility data (χ_M) per complex molecule and effective magnetic moment per nickel(II) ion (μ_{eff}) *vs* temperature for **3**. The solid lines result from a least-squares fit to the theoretical eq 1 given in the text.

0.03−0.07 Å. The two metal centers are not coplanar, the dihedral angle between their mean planes is 34.4(1)°. As a result of the acetate bridging the macrocycle is distorted to such an extent that the two phenyl rings are inclined to each other by 60.0(2)°. The orientations of the acetate plane with respect to the two metal planes are somewhat different, 72.6(3) and 80.2(2)°. The nickel atoms are separated by 3.043(4) Å with twounequal Ni−O−Ni bridge angles, 90.6(3) and 95.1(2)°. The average Ni−N distance (2.09(1) Å) is similar to the other high-spin nickel(II) complexes of H_2L.[17,19,29] However, the Ni−O(phenoxy) distances, which are unequal and vary between 2.059(4) and 2.158(4) Å, are considerably longer relative to those of other complexes,[17,19,29] Å, are considerably longer relative to those of other complexes,[17,19,29] for which the average Ni−O distance is 2.02(1) Å. Interestingly, the carboxylate Ni−O distances (average 2.055(8) Å) are appreciably shorter than the Ni−OH_2 distances (average 2.150(4) Å). In complex **2** there are a few intra- and intermolecular hydrogen bonds involving the coordinated water molecules, NH groups, and ClO_4^- ions.

Table 5. Bond Distances (Å) and Angles (deg) Relevant to the Ni Coordination Spheres in $[Ni_2L(\mu\text{-}O_2CCH_3)(H_2O)_2](ClO_4)\cdot CH_3OH\cdot H_2O$ (**2**)

Ni(1)−O(9)	2.059(4)	Ni(6)−O(9)	2.064(4)
Ni(1)−O(31)	2.158(4)	Ni(6)−O(31)	2.124(4)
Ni(1)−O(2)	2.048(4)	Ni(6)−O(5)	2.064(4)
Ni(1)−O(8)	2.146(4)	Ni(6)−O(7)	2.153(5)
Ni(1)−N(18)	2.082(6)	Ni(6)−N(33)	2.090(5)
Ni(1)−N(22)	2.089(6)	Ni(6)−N(37)	2.106(5)
Ni(1)···Ni(6)	3.043		
Ni(1)−O(9)−Ni(6)	95.1(2)	O(31)−Ni(1)−N(22)	91.9(2)
Ni(1)−O(31)−Ni(6)	90.8(3)	O(31)−Ni(6)−N(33)	94.0(2)
O(9)−Ni(1)−O(31)	81.9(2)	O(2)−Ni(1)−O(8)	175.7(2)
O(9)−Ni(6)−O(31)	82.4(2)	O(5)−Ni(6)−O(7)	176.5(2)
N(22)−Ni(1)−N(18)	91.1(2)	O(2)−C(3)−O(5)	125.6(5)
N(33)−Ni(6)−N(37)	90.4(2)	Ni(1)−O(2)−C(3)	129.8(5)
O(9)−Ni(1)−N(18)	95.1(2)	Ni(6)−O(5)−C(3)	125.5(3)
O(9)−Ni(6)−N(37)	93.5(2)		

Magnetochemistry. The variable-temperature (5−300 K) magnetic susceptibility data were collected for complexes **1**−**5**. The χ_M *vs* T values for **1**−**3** are illustrated in Figures 5−7. It may be noted that in all the cases the χ_M values increase slowly with the decrease of temperature, but in the low temperature region rapid increase of the molar susceptibility values occur without showing a peak. This trend indicates that the overall exchange interaction between the two metal centers is weak, although the sign of J is not evident. Assuming an isotropic model, the exchange expression for two equivalent $S = 1$ ions based on the spin Hamiltonian, $H = 2JS_1 \cdot S_2$, is given by

$$\chi_M = \frac{N\beta^2 g^2}{kT}\left[\frac{10 + 2\exp(-4J/kT)}{5 + 3\exp(-4J/kT) + \exp(-6J/kT)}\right](1-\varrho) + \frac{2N\beta^2 g^2 \varrho}{3kT} + N_\alpha \quad (1)$$

The symbols N, β, g, and k have their usual meanings, ϱ represents the fraction of paramagnetic impurity, and $N_\alpha = 8N\beta^2/10Dq$ is the temperature-independent paramagnetism.

Least-squares fittings of eq 1 to the experimental data for complexes **1** and **3** are illustrated in Figures 5 and 7, respectively. The relevant magnetic parameters thus obtained for complexes **1**−**5** are given in Table 6. In the case of complex **2** the effect of zero-field splitting parameter (D) of nickel(II) ions and interdimer exchange parameters (zJ') on the intramolecular exchange parameter (J) have also been considered. The

(29) (a) Nanda, K. K.; Das, R.; Venkatsubramanian, K.; Paul, P.; Nag, K. *J. Chem. Soc., Dalton Trans.* **1993**, 2515. (b) Nanda, K. K.; Das, R.; Newlands, M. J.; Hynes, R.; Gabe, E. J.; Nag, K. *J. Chem. Soc., Dalton Trans.* **1992**, 897.

Table 6. Magnetic Data for Complexes **1**–**6**

complex	J, cm^{-1}	g	ϱ^a	10^2R^b
$[Ni_2L(\mu\text{-}O_2CH)(H_2O)_2](ClO_4)$ (**1**)	−0.7	2.24	0	1.52
$[Ni_2L(\mu\text{-}O_2CCH_3)(H_2O)_2](ClO_4)\cdot CH_3OH\cdot H_2O$ (**2**)	2.9	2.17	0.06	2.91
$[Ni_2L(\mu\text{-}O_2CCH_2CH_3)(H_2O)_2](ClO_4)\cdot 2CH_3CH_2CO_2H$ (**3**)	2.2	2.15	0.08	2.02
$[Ni_2L(\mu\text{-}O_2CCH_2CH_2CH_3)(H_2O)_2](ClO_4)\cdot 2CH_3CH_2CH_2CO_2H$	0.5	2.23	0.08	2.88
$[Ni_2L(\mu\text{-}O_2CC_6H_5)(H_2O)_2](ClO_4)\cdot 2C_6H_5CO_2H$ (**5**)	5.0	2.14	0.05	2.71
$[Ni_2L(\mu\text{-}O_2CCH_2NH_3)(H_2O)_2](ClO_4)\cdot 2H_2O$ (**6**)	−1.1	2.21	0.0002	2.25

[a] Fraction of paramagnetic impurity. [b] $R = [\Sigma(\chi_{obs} - \chi_{calc})^2/\Sigma\chi_{obs}^2]^{1/2}$.

Table 7. Comparison of Magnetostructural Data in Mono, Double, and Triple Carboxylate-Bridged Complexes

complex cation	Ni···Ni, Å	Ni−O−Ni, deg	J, cm^{-1}	ref
$[Ni_2(tmen)_2(\mu\text{-}H_2O)_2(\mu\text{-}O_2CCH_3)]^{2+}$ [a]	3.56	117.2	<0[b]	12
$[Ni_2(tmen)_2(\mu\text{-}O_2CCH_3)_3(urea)]^+$ [a]	3.47		−0.9	16
$[Ni_2(Me_3tacn)(\mu\text{-}OH)(\mu\text{-}O_2CCH_3)_2]^+$ [c]	3.40	115.2	−4.5	13
$[Ni_2(bimp)(\mu\text{-}O_2CCH_3)_2]^+$ [d,e]	3.42	116.7	−1.9	14
$[Ni_2(bpmp)(\mu\text{-}O_2CCH_3)_2]^+$ [d,f]			−1.2	15
$[Ni_2L(\mu\text{-}O_2CCH_2NH_3)(H_2O)_2]^{2+}$	3.07	95.0, 92.6	−1.1	17a
$[Ni_2L(\mu\text{-}O_2CCH_3)(H_2O)]^+$	3.04	95.1, 90.8	2.9	this work

[a] tmen = *N,N,N′,N′*-tetramethylethylenediamine. [b] Estimated as $-2 < J < 0$. [c] Me_3tcan = *N,N′,N″*-trimethyl-1,4,7-triazacyclanonane. [d] Phenoxy-bridged compound. [e] Hbimp = 2,6-bis[bis((1-methylimidazol-2-yl)methyl)amino)methyl]-4-methylphenol. [f] Hbpmp = 2,6-bis[bis(2-pyridylmethyl)amino)methyl]-4-methylphenol.

magnetic susceptibility expression[30] in this case is given by eq 2. Nonlinear least-squares fitting of the above expression for

$$\chi_M = \chi(g, J, D, zJ')(1 - \varrho) + 2N\beta^2g^2\varrho/3kT + N_\alpha \quad (2)$$

complex **2** is shown in Figure 6. It should be noted that the values of $J = 3.05$ cm^{-1}, $g = 2.18$, $D = 1.6$ cm^{-1}, and $zJ' = 0.04$ cm^{-1} thus obtained for **2** do not differ significantly from the values of $J = 2.94$ cm^{-1} and $g = 2.17$ obtained by using eq 1. This again supports that the estimation of J is weakly correlated[31] with D and zJ'. Thus, the J values of the complexes (Table 6) appear accurately determined.

In contrast to the χ_M *vs* T plots of complexes **1**–**3** corresponding μ_{eff} (per Ni^{2+}) *vs* T plots (Figures 5–7), however, clearly indicate the sign of J. The data given in Table 6 show that except for **1**, which exhibits antiferromagnetic interaction ($J = -0.7$ cm^{-1}), the other four complexes behave ferromagnetically with the values of J varying between 0.5 and 5 cm^{-1}.

The structure[32] and magnetic property[17a] of the glycinate complex, $[Ni_2L(\mu\text{-}O_2CCH_2NH_3)(H_2O)_2](ClO_4)_2\cdot 2H_2O$ (**6**), may be compared with the present series of compounds. In **6** unusual carboxylate bridging occurs due to the involvement of zwitterionic glycine. The nickel(II) ions in **6**, similar to **1**, are antiferromagnetically coupled ($J = -1.1$ cm^{-1}). A comparison of the structural parameters of **2** and **6** discloses that aside from small differences in the bond distances and angles pertaining to the nickel coordination spheres, there is significant difference in the orientation of the carboxylate moieties with respect to the metal centers. In **6** the plane of the carboxylate group is almost orthogonally disposed to the mean planes of the two nickel centers, 92.6(4) and 90.0(4)°, while in the case of **2** these dihedral angles are 72.6(3) and 80.0(2)°. The two compounds also differ in their Ni−O−Ni phenoxy bridge angles in the following way: 90.8(3) and 95.1(2)° for **2** and 92.6(3) and 95.0(3)° for **6**.

As already mentioned that for a series of octahedral and square pyramidal dinickel(II) complexes of H_2L with centrosymmetric structures there exists a linear relationship[17b] between the values of J and Ni−O−Ni bridge angles or Ni···Ni distances. Exchange coupling in these compounds occur only through the equatorial plane and inversion from antiferromagnetic to ferromagnetic coupling is anticipated at a bridge angle of 97°. A similar trend, involving J and Ni−O−Ni angle or Ni···Ni distance, is not expected for complexes **1**–**6** because not only do they provide two different pathways (axial and equatorial) for exchange coupling but also the equatorial pathway involves two noncoplanar metal centers. Clearly, exchange interaction behaviors of these compounds are quite complicated. Nevertheless, consideration of the overall exchange interaction in terms of a single J parameter, an approach also adopted by others[13–16] for carboxylate-bridged dinickel(II) complexes, provides an insight to magnetostructural relationship in these compounds. We note that J_{eff} ($J_{AF} + J_F$) is dependent on the angle of inclination of the carboxylate plane to the metal planes. J_F seems to prevail over J_{AF} when these dihedral angles deviate from 90° to lower values.

The magnetostructural parameters for the known doubly- and triply-bridged carboxylate complexes[12–16] are listed in Table 7. All of these complexes exhibit weak antiferromagnetic interaction. However, the J values show no correlation either with Ni···Ni distance or Ni−O−Ni angle involving an aqua, hydroxy, or phenoxy bridge. The present series of diphenoxy monocarboxylate-bridged complexes, similar to the above compounds, also exhibit weak exchange interactions. Additionally, this study has demonstrated for the first time that by varying the carboxylate bridge in nickel(II) complexes it is possible to tilt the balance to favor either ferromagnetic or antiferromagnetic coupling.

Acknowledgment. K.N. is grateful to SERC of the Department of Science and Technology of Government of India for financial support to this research and L.K.T. to the Natural Sciences and Engineering Research Council of Canada for support for the variable-temperature magnetic susceptibility facility.

Supplementary Material Available: Tables I–IV, giving of anisotropic thermal parameters, hydrogen atom positions, complete bond distances and angles, and least-squares planes for complex **2** (10 pages). Ordering information is given on any current masthead page.

(30) Ginsberg, A. P.; Martin, R. L.; Brookes, R. W.; Sherwood, R. C. *Inorg. Chem.* **1972**, *11*, 2884.
(31) Duggan, M. D.; Barefield, E. K.; Hendrickson, D. N. *Inorg. Chem.* **1973**, *12*, 985.
(32) Das, R.; Nanda, K. K.; Venkatsubramanian, K.; Paul, P.; Nag, K. *J. Chem. Soc., Dalton Trans.* **1992**, 1253.